known that retinoic acid, a compound related to vitamin A, can activate homeobox genes (reviewed in ref. 13); our results may be evidence of a vitamin A-mediated induction of homeobox genes for limb formation. □

Received 26 July; accepted 4 November 1991.

1. Niazi, I. A. & Saxena, S. *Experientia* **24,** 852–853 (1968).
2. Niazi, I. A. & Saxena, S. *Indian J. exp. Biol.* **17,** 866–868 (1979).
3. Maden, M. *J. Embryol. exp. Morphol.* **77,** 273–295 (1983).
4. Maden, M., Keeble, S. & Cox, R. A. *Roux's Arch. dev. Biol.* **194,** 228–235 (1985).
5. Scadding, S. R. & Maden, M. *J. Embryol. exp. Morphol.* **91,** 19–34 (1986).
6. Scadding, S. R. & Maden, M. *J. Embryol. exp. Morphol.* **91,** 35–53 (1986).
7. Ludolph, D. C., Cameron, J. A. & Stocum, D. L. *Devl. Biol.* **140,** 41–52 (1990).
8. Thomas, S. D. & Stocum, D. *Devl Biol.* **103,** 319–328 (1984).
9. Niazi, I. A. & Alam, S. *Roux's Arch. dev. Biol.* **193,** 111–116 (1984).
10. Tickle, C., Alberts, B., Walpert, L. & Lee, J. *Nature* **296,** 564–566 (1982).
11. Summerbell, D. *J. Embryol. exp. Morphol.* **78,** 269–289 (1983).
12. Mohanty-Hejmadi, P. *Prakruti-Utkal Univ. J. Sci.* **11,** 81–87 (1977).
13. De Robertis, E. M., Oliver, G. & Wright, C. V. E. *Scient. Am.* 46–52 (July, 1990).

ACKNOWLEDGEMENTS. P.M. thanks the University Grants Commission for a junior research fellowship.

Depletion of intracellular calcium stores activates a calcium current in mast cells

Markus Hoth & Reinhold Penner

Max-Planck-Institut für biophysikalische Chemie, Am Fassberg, 3400 Göttingen, Germany

In many cell types, receptor-mediated Ca^{2+} release from internal stores is followed by Ca^{2+} influx across the plasma membrane[1–3]. The sustained entry of Ca^{2+} is thought to result partly from the depletion of intracellular Ca^{2+} pools[4,5]. Most investigations have characterized Ca^{2+} influx indirectly by measuring Ca^{2+}-activated currents[6–9] or using Fura-2 quenching by Mn^{2+}, which in some cells enters the cells by the same influx pathway[10,11]. But only a few studies have investigated this Ca^{2+} entry pathway more directly[12–14]. We have combined patch-clamp and Fura-2 measurements to monitor membrane currents in mast cells under conditions where intracellular Ca^{2+} stores were emptied by either inositol 1,4,5-trisphosphate, ionomycin, or excess of the Ca^{2+} chelator EGTA. The depletion of Ca^{2+} pools by these independent mechanisms commonly induced activation of a sustained calcium inward current that was highly selective for Ca^{2+} ions over Ba^{2+}, Sr^{2+} and Mn^{2+}. This Ca^{2+} current, which we term I_{CRAC} (calcium release-activated calcium), is not voltage-activated and shows a characteristic inward rectification. It may be the mechanism by which electrically nonexcitable cells maintain raised intracellular Ca^{2+} concentrations and replenish their empty Ca^{2+} stores after receptor stimulation.

We have perfused inositol 1,4,5-trisphosphate ($Ins(1,4,5)P_3$) (10 μM) into mast cells through patch pipettes under conditions where Ca^{2+} currents are likely to be large, that is, clamping the cytosol to low intracellular Ca^{2+} concentrations ($[Ca^{2+}]_i$) using EGTA (10 mM) and increasing extracellular Ca^{2+} concentration ($[Ca^{2+}]_o$) (10 mM). Figure 1*a* illustrates that shortly after rupturing the patch that established continuity between patch pipette and cytosol (whole-cell configuration), a sustained inward current developed while the cell's membrane potential was clamped to 0 mV. The activation of the inward current by $Ins(1,4,5)P_3$ was observed in 111 out of 115 cells. The time course of the current was very similar in all the cells in which $Ins(1,4,5)P_3$ activated it, with delays following patch rupture of 7 ± 1 s (mean ± s.e.m., $n = 14$) and times from onset to half-maximal activation of 11 ± 1 s (mean ± s.e.m., $n = 12$). Because $Ins(1,4,5)P_3$-induced Ca^{2+} release starts within 1 s of establishment of the whole-cell configuration[12,15], the delay in the appearance of the Ca^{2+} current indicates that $Ins(1,4,5)P_3$ is not likely

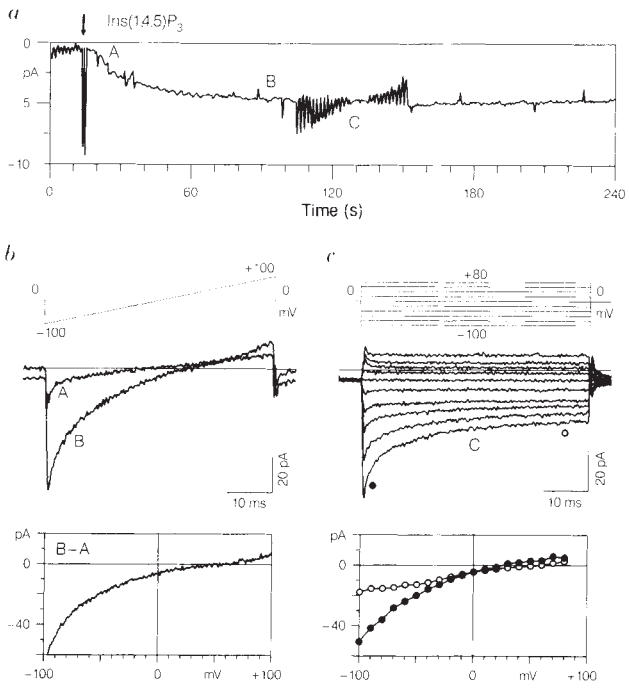

FIG. 1 Activation of the Ca^{2+} current by $Ins(1,4,5)P_3$. All data shown are taken from a single cell representative of a total of more than 100 similar experiments. *a*, Temporal pattern of activation of an inward current recorded at 0 mV holding potential during perfusion with the standard pipette solution supplemented with $Ins(1,4,5)P_3$ (10 μM) and EGTA (10 mM). Establishment of the whole-cell mode is indicated by the arrow. Data were sampled at 2 Hz. Immediately after breaking the patch, voltage ramps as shown in *b* were applied (occasionally sampled and seen as little spikes in the current trace). Labels A and B indicate times at which high-resolution current traces were taken for display in *b*, whereas C refers to traces obtained by square pulses shown in *c*. *b*, Single high-resolution current traces before (A) and after (B) development of the inward current. The voltage-ramp protocol is schematically shown on top. The lower graph illustrates the current–voltage relationship of the inward current as obtained by subtracting pooled leak-current ramps as in A from pooled steady-state current ramps as in B. *c*, Family of high-resolution current traces obtained after development of the inward current (C). The voltage-pulse protocol is schematically shown on top. The lower graph illustrates the current–voltage relationships taken at the times indicated by the circles (●, 0.5 ms; ○, 45 ms after the pulse). The data points were corrected by subtracting a linear leak current that was estimated from the slope of the ramp currents obtained before appearance of the inward current.

METHODS. Rat peritoneal mast cells were isolated and cultured as described[26]. Patch-clamp experiments were done in the tight-seal whole-cell configuration at 23–27 °C in standard saline solution containing (in mM): NaCl, 140; KCl, 2.8; $CaCl_2$, 10; $MgCl_2$, 2; glucose, 11; HEPES-NaOH, 10, pH 7.2. Sylgard-coated patch pipettes had resistances between 2.5–5 MΩ after filling with the standard intracellular solution which contained (in mM): potassium-glutamate, 145; NaCl, 8; $MgCl_2$, 1; Fura-2, 0.1; Mg-ATP, 0.5; EGTA, 10; HEPES-KOH, 10, pH 7.2. $Ins(1,4,5)P_3$ (10 μM, Amersham) and heparin (500 μg ml^{-1}; low M_r, from Sigma) were added to this solution when needed. Extracellular solution changes were made by local application from a wide-tipped micropipette. These pipettes contained the standard saline supplemented with ionomycin (10 μg ml^{-1}, Calbiochem) or, in the case of ion-substitution experiments, equimolar concentrations of $BaCl_2$, $SrCl_2$ or $MnCl_2$ in exchange for 10 mM $CaCl_2$. Possible contaminations of Ca^{2+} were chelated by the addition of EGTA (1 mM). The $[Ca^{2+}]_i$ was monitored with a photomultiplier-based system as described[27]. The fluorescent indicator dye Fura-2 was loaded by diffusion from the patch pipette. $[Ca^{2+}]_i$ was calculated from the fluorescence ratio (360/390 nm) based on a calibration procedure as described[27]. The two fluorescence intensities, DC current, and DC voltage were sampled at 2 Hz and filtered at 500 Hz. In addition, high-resolution current recordings were acquired by a computer-based patch-clamp amplifier system (EPC-9). Capacitive currents and series resistance were cancelled before each voltage ramp using the automatic capacitance compensation of the EPC-9. Currents were filtered at 2.3 kHz and digitized at 100 μs intervals. For analysis, currents were filtered digitally to 1 kHz.

to gate the current directly but rather secondarily, following depletion of intracellular Ca^{2+} stores.

To obtain current-voltage relationships for the current, we intermittently applied short (50 ms) voltage ramps from −100 to +100 mV (occasionally seen as spikes in the current trace of Fig. 1*a*). The very first ramps (labelled A in Fig. 1*a*) produced essentially a linear leak current (trace A in Fig. 1*b*). Subsequent ramps showed a gradually increasing inwardly rectifying current over almost the entire voltage range (trace B in Fig. 1*b*). The net current activated by $Ins(1,4,5)P_3$ in this experiment is obtained when subtracting trace A from trace B (current-voltage relationship in Fig. 1*b*). The rather positive reversal potential of the current suggests specificity for Ca^{2+} ions as charge carriers. The apparent reversal of the current at about +50 mV is probably underestimated, as mast cells have chloride currents which develop under many experimental conditions[12,16], and which often prevented an accurate assessment of the Ca^{2+} current at very positive potentials.

We tested whether the strong inward rectification at negative potentials is a genuine property of the inward current or caused by the ramp protocol. This was done by applying square voltage pulses over the same voltage range (Fig. 1*c*). The current responses to negative voltage pulses, where Ca^{2+} influx is largest, show some inactivation. Most of this inactivation is presumably Ca^{2+}-induced, as in preliminary experiments with the fast Ca^{2+} chelator BAPTA (1,2-bis(*O*-aminophenoxy)ethane-*N*,*N*,*N*′,*N*′-tetraacetic acid), the inactivation was attenuated (data not shown). It thus seems that even 10 mM EGTA cannot buffer the incoming Ca^{2+} fast enough to prevent the inactivation. Both Ca^{2+}-induced inactivation and the ineffectiveness of EGTA in preventing it are also characteristic of voltage-activated Ca^{2+} channels[17]. The current-voltage relationships of the currents taken at the beginning and the end of each voltage pulse are depicted in Fig. 1*c*. When comparing these with the *I*–*V* curves obtained by voltage ramps, we conclude that the ramp protocol yields an appropriate representation of the current's behaviour, well aware of the fact that the ramp *I*–*V* curves just slightly exaggerate the curvature at negative potentials because of the Ca^{2+}-induced inactivation.

Although $Ins(1,4,5)P_3$ in conjunction with EGTA was the strongest activator of the Ca^{2+} current it seems unlikely that $Ins(1,4,5)P_3$ activated the current directly. This is corroborated by the finding that simply omitting the $Ins(1,4,5)P_3$ from the pipette solution, but leaving the high concentration of EGTA (10 mM), often resulted in activation of a Ca^{2+} current that was qualitatively indistinguishable from the $Ins(1,4,5)P_3$-induced conductance (Fig. 2*a*). This EGTA-induced activation was less reliable (21 out of 49 cells) and the delays as well as the times from onset to half-maximal activation were significantly longer compared with those of $Ins(1,4,5)P_3$ (mean delay after establishment of the whole-cell configuration: 44 ± 9 s, s.e.m., $n = 13$; mean time for half-maximal activation: 34 ± 9 s, s.e.m., $n = 10$). The range of responses is illustrated in Fig. 2*a*. EGTA could also activate I_{CRAC} in cells where large concentrations of heparin were added to the pipette solution (seven cells). Under these conditions, possible effects of $Ins(1,4,5)P_3$ should have been blocked[18]. We conclude the EGTA may empty intracellular Ca^{2+} stores by increasing the concentration gradients between cytosol and Ca^{2+} stores and prevents the refilling by acting as a scavenger. Under these conditions, it should mainly depend on how full and how 'leaky' the internal stores are, and whether, when and to what degree the influx pathway is activated.

Thapsigargin (1 μg ml^{-1}), a blocker of the Ca^{2+} pump of the endoplasmic reticulum[19], could not induce activation of the Ca^{2+} current in cells where EGTA failed to do so (data not shown). This result is not unexpected, because the actions of thapsigargin should be equivalent to those of EGTA, namely preventing the reuptake of released Ca^{2+} into the stores. In the absence of intracellular EGTA, thapsigargin caused a rapid and sustained increase in $[Ca^{2+}]_i$ from basal levels of 312 ± 62 nM to 1,013 ± 120 nM (means ± s.e.m., $n = 6$). Part of this response was due to Ca^{2+} entry, probably through minimal activation of I_{CRAC}, which could not be resolved as its amplitude was less than 2 pA at −40 mV (data not shown). Again this is not unexpected, as under these unbuffered conditions the increase in $[Ca^{2+}]_i$ may prevent full activation of I_{CRAC} by reducing the driving force for both Ca^{2+} release and Ca^{2+} entry. In addition, elevated $[Ca^{2+}]_i$ may cause substantial inactivation of I_{CRAC}.

An efficient way of depleting intracellular stores is by applying ionomycin[20]. Figure 2*b* illustrates an example of a cell in which EGTA did not activate the Ca^{2+} current and heparin was present to prevent a possible increase in $Ins(1,4,5)P_3$ formation. Subsequent application of ionomycin (10 μg ml^{-1}) induced an increase in $[Ca^{2+}]_i$ and the activation of I_{CRAC}, which in all

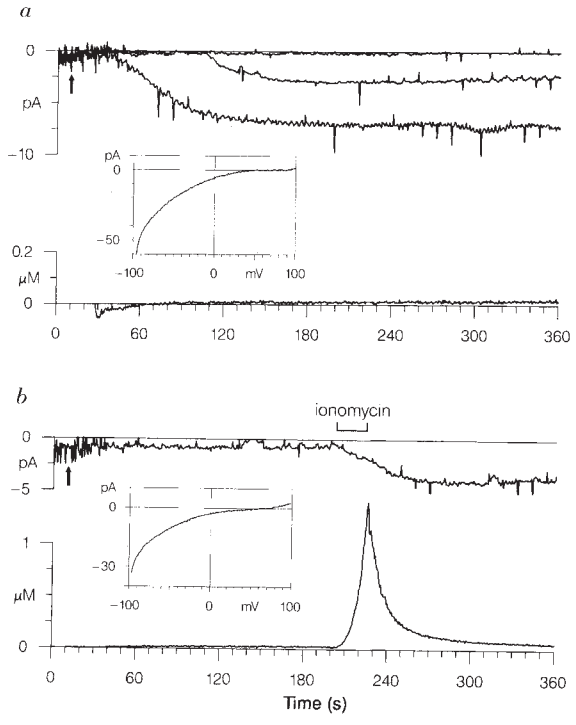

FIG. 2 Activation of the Ca^{2+} current by EGTA and ionomycin. *a*, Temporal pattern of activation of inward currents recorded at 0 mV holding potential during perfusion with the standard pipette solution which contained 10 mM EGTA. The superimposed current traces represent three different cells and demonstrate the range of observed responses. The bottom trace corresponds to $[Ca^{2+}]_i$ of the experiment with the largest current. In this experiment, which also showed the fastest time course of activation of all cells in this series, the pipette solution also contained heparin (500 μg ml^{-1}). The inset shows the current-voltage relationship of that current after full development (leak-corrected as described in Fig. 1*b*). *b*, Experimental conditions as in *a*. This cell did not develop an inward current in the presence of EGTA. It was, however, induced by application of ionomycin (10 μg ml^{-1}) at the time indicated.

cases strictly correlated with the administration of the ionophore (17 out of 17 cells). The $[Ca^{2+}]_i$ increase is probably due to translocation of $[Ca^{2+}]_o$ across the plasma membrane and is so large that it overwhelms the buffering capacity of EGTA. Ionomycin also releases Ca^{2+} from internal stores and this presumably activates the Ca^{2+} current. It is unlikely that the current is induced by ionomycin itself as the ionophore is thought to translocate Ca^{2+} by an electroneutral carrier mechanism[21]. Moreover, we have seen similar changes in $[Ca^{2+}]_i$, but have not detected additional current components associated with the application of ionomycin in cells in which the current was already fully activated by $Ins(1,4,5)P_3$ (12 out of 12 cells).

We assessed the specificity of this influx pathway by activating it with $Ins(1,4,5)P_3$ and EGTA-containing pipette solutions and have subsequently removed extracellular Ca^{2+}. This abolished the inward current (Fig. 3*a*), suggesting that the current is specific for divalent ions. Most Ca^{2+} channels known are highly permeant to Ba^{2+} and Sr^{2+}. But I_{CRAC} seems not to be carried by these ions. Figure 3*b* shows that the equimolar substitution of extracellular Ca^{2+} by Ba^{2+} and addition of 1 mM EGTA clearly reduces the inward current. This effect of Ba^{2+} was observed in five out of five cells and similar results were obtained with Sr^{2+} (two out of two cells). It is not yet clear whether Ba^{2+} is impermeable or the Ca^{2+} influx pathway requires Ca^{2+} at the extracellular side to function. Another possible explanation for the reduction in Ca^{2+} current could be an inactivation of the current from the inside by an initial entry of Ba^{2+} into the cell. In Fig. 3*b* there is an increase in the fluorescence-ratio trace which may be attributed to Ba^{2+} entering the cytosol and affecting Fura-2 fluorescence. We noticed that the increase in the ratio was due to an increase in the fluorescence at 360 nm excitation (isostilbic point of Fura-2 for Ca^{2+}) and a decrease in fluorescence at 390 nm excitation (data not shown). This suggests that the isostilbic point of Fura-2 with respect to Ba^{2+} is shifted to longer wavelengths and may be used to monitor Ba^{2+} fluxes in cells where $[Ca^{2+}]_i$ is strongly buffered by EGTA.

In some cell types Mn^{2+} seems to permeate through the same Ca^{2+} influx pathway as Ca^{2+} does[10,22-24] (but see ref. 25). With as little as 50 μM of extracellular Mn^{2+}, its entry can be measured by a large quench of Fura-2 fluorescence in the cytosol[11]. We have therefore substituted extracellular Ca^{2+} by 10 mM Mn^{2+} and added 1 mM EGTA. When applying this solution to a cell that had developed a Ca^{2+} current, there was a strong block of the current and a concommitant decrease in $[Ca^{2+}]_i$ (Fig. 3*c*). However, there was only a very small decrease in the fluorescence signal obtained at 360 nm excitation, suggesting little if any Mn^{2+} entry through the influx pathway. This would suggest that in other cell types Mn^{2+} can enter through other pathways (for example receptor-operated channels or ion transporters), or that Mn^{2+} entry occurs through a similar current as described here with a different selectivity for divalent ions.

We have shown that depleting intracellular Ca^{2+} stores by three independent mechanisms activates a highly selective inwardly rectifying Ca^{2+} current in mast cells. As ionomycin and EGTA can activate I_{CRAC} in the presence of heparin, we do not find that inositol phosphates ($Ins(1,4,5)P_3$ or $Ins(1,3,4,5)P_4$) are necessary for activating calcium influx (as proposed in ref. 2). The characteristics of this current are different from classic voltage-activated Ca^{2+} currents in that Ba^{2+} and Sr^{2+} do not seem to permeate this pathway readily. At present, we do not know how the emptying of the intracellular Ca^{2+} stores translates into activation of a plasma membrane current. This might be due to a second messenger released from the storage organelles or a direct coupling between proteins in the two membranes. □

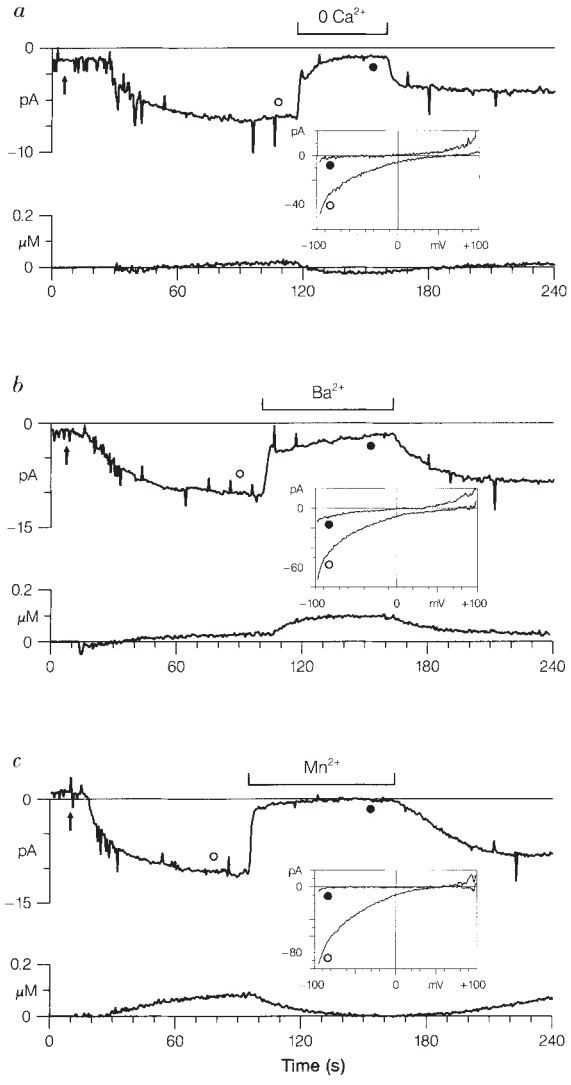

FIG. 3 Permeability of the inward current to divalent cations. In all three experiments the Ca^{2+} current was activated by pipette solutions containing $Ins(1,4,5)P_3$ (10 μg ml^{-1}) and EGTA (10 mM). The upper traces correspond to currents sampled at 0 mV and bottom traces show $[Ca^{2+}]_i$. The insets correspond to current–voltage relationships derived from subtracting pooled ramps shortly after break-in (before activation of the current) from pooled current responses at the times indicated by the respective symbols (○, inward current at 10 mM Ca^{2+}, ●, current during application of test solution). *a*, standard saline (10 mM Ca^{2+}) was changed to Ca^{2+}-free saline (1 mM EGTA added). *b*, Equimolar substitution of 10 mM Ca^{2+} in standard saline by 10 mM Ba^{2+} (1 mM EGTA added). *c*, Equimolar substitution of 10 mM Ca^{2+} in standard saline by 10 mM Mn^{2+} (1 mM EGTA added).

Received 12 August; accepted 4 October 1991.

1. Berridge, M. J. & Irvine, R. F. *Nature* **341,** 197–205 (1989).
2. Irvine, R. F. *FEBS Lett.* **263,** 5–9 (1990).
3. Meldolesi, J., Clementi, E., Fasolato, C., Zacchetti, D. & Pozzan, T. *Trends pharmacol. Sci.* **12,** 289–292 (1991).
4. Casteels, R. & Droogmans, G. *J. Physiol., Lond.* **317,** 263–279 (1981).
5. Putney, J. W. Jr *Cell. Calcium* **11,** 611–624 (1990).
6. Bird, G. St J. *et al. Nature* **352,** 162–165 (1991).
7. Morris, A. P., Gallacher, D. V., Irvine, R. F. & Petersen, O. H. *Nature* **330,** 653–655 (1987).
8. Liano, I., Marty, A. & Tanguy, J. *Pflügers Arch.* **409,** 499–506 (1987).
9. Snyder, P. M., Krause, K.-H. & Welsh, M. J. *J. biol. Chem.* **263,** 11048–11051 (1988).
10. Sage, S. O., Merritt, J. E., Hallam, T. J. & Rink, T. J. *Biochem. J.* **258,** 923–926 (1989).
11. Jacob, R. *J. Physiol., Lond.* **421,** 55–77 (1990).
12. Penner, R., Matthews, G. & Neher, E. *Nature* **334,** 499–504 (1988).
13. Matthews, G., Neher, E. & Penner, R. *J. Physiol., Lond.* **418,** 105–130 (1989).
14. Lewis, R. S. & Cahalan, M. D. *Cell Regulation* **1,** 99–112 (1989).
15. Marty, A. & Tan, Y. P. *J. Physiol., Lond.* **419,** 665–687 (1989).
16. Matthews, G., Neher, E. & Penner, R. *J. Physiol., Lond.* **418,** 131–144 (1989).
17. Eckert, R. & Chad, J. E. *Prog. Biophys. molec. Biol.* **44,** 215–267 (1984).
18. Cullen, P. J., Comerford, J. G. & Dawson, A. P. *FEBS Lett.* **228,** 57–59 (1988).
19. Thastrup, O., Cullen, P. J., Drobak, B. K., Hanley, M. R. & Dawson, A. P. *Proc. natn. Acad. Sci. USA* **87,** 2466–2470 (1990).
20. Albert, P. R. & Tashjian, A. H. Jr *J. biol. Chem.* **259,** 15350–15363 (1984).
21. Liu, C. & Hermann, T. E. *J. biol. Chem.* **253,** 5892–5894 (1978).
22. Merritt, J. E., Jacob, R. & Hallam, T. J. *J. biol. Chem.* **253,** 1522–1527 (1989).
23. Mertz, L. M., Baum, B. J. & Ambudkar, I. S. *J. biol. Chem.* **265,** 15010–15014 (1990).

24. Kass, G. E. N., Llopis, J., Chow, S. C., Duddy, S. K. & Orrenius, S. *J. biol. Chem.* **265,** 17486–17492 (1990).
25. Llopis, J., Chow, S. B., Kass, G. E. N., Gahm, A. & Orrenius, S. *Biochem. J.* **277,** 553–556 (1991).
26. von zur Mühlen, F., Eckstein, F. & Penner, R. *Proc. natn. Acad. Sci. U.S.A.* **88,** 926–930 (1991).
27. Neher, E. in *Neuromuscular Junction* (eds Sellin, L. C., Libelius, R. & Thesleff, S.) 65–76 (Elsevier, Amsterdam, 1989).

ACKNOWLEDGEMENTS. We thank E. Neher for critical comments on the manuscript. This work was supported in part by the Deutsche Forschungsgemeinschaft and the Sonderforschungsbereich 236.

Inositol 1,3,4,5-tetrakisphosphate activates an endothelial Ca^{2+}-permeable channel

Andreas Lückhoff & David E. Clapham

Department of Pharmacology, Mayo Foundation, Rochester, Minnesota 55905, USA

RECEPTOR-MEDIATED increases in the cytosolic free calcium ion concentration in most mammalian cells result from mobilization of Ca^{2+} from intracellular stores as well as transmembrane Ca^{2+} influx. Inositol 1,4,5-trisphosphate ($InsP_3$) releases calcium from intracellular stores[1] by opening a Ca^{2+}-permeable channel in the endoplasmic reticulum[2–4]. But the mechanism and regulation of Ca^{2+} entry into nonexcitable cells has remained elusive because the entry pathway has not been defined. Here we characterize a novel inositol 1,3,4,5-tetrakisphosphate ($InsP_4$) and Ca^{2+}-sensitive Ca^{2+}-permeable channel in endothelial cells. We find that $InsP_4$, which induces Ca^{2+} influx into acinar cells[5,6], enhances the activity of the Ca^{2+}-permeable channel when exposed to the intracellular surface of endothelial cell inside-out patches. Our results suggest a molecular mechanism which is likely to be important for receptor-mediated Ca^{2+} entry.

Manganese ions may use the same entry pathway as Ca^{2+} in stimulated endothelial cells[7,8]. To quantify Mn^{2+} influx, endothelial cells patch-clamped with the nystatin technique[9] and stimulated with ATP (30 μM) were exposed to Mn^{2+}(6 mM). Figure 1 shows that at negative membrane potentials, close to the potassium equilibrium potential (E_K), an inward current of 40 ± 24(±s.d., $n = 8$) pA (3.2 ± 2.5 pA pF^{-1}) was activated by ATP. No such Mn^{2+} current was observed in unstimulated cells (not shown) or in depolarized cells, in accordance with previous reports that endothelial cation influx is inhibited by depolarization[10–12].

Using patch-clamp techniques[13], Mn^{2+}-permeant single channels were identified in cell-attached, inside-out and outside-out patches. For these experiments, Mn^{2+} (110 or 140 mM) was used as the dominant charge carrier. Channel events observed in inside-out patches are shown in Fig. 2*a*. Channel activity was observed at membrane potentials ranging from −160 to −10 mV, with a slope conductance of 2.5 pS and a mean open time of about 230 ms at −80 mV. The low single-channel conductance prevented rigorous analysis of the channel kinetics. Glutamate replacement of chloride in the bath did not affect channel conductance. When Ca^{2+} or Ba^{2+} replaced Mn^{2+} in the pipette, no measurable change in the conductance from −120 to −60 mV was noted, suggesting that the channel is roughly equally permeable to these divalent cations. The channel was more selective for divalent than sodium ions (>2:1) as shown in outside-out patch experiments ($n = 3$; Fig. 2*d*) but determination of absolute permeability ratios is prohibited by the low channel conductance in realizable ionic concentrations.

Typically, inside-out patches exhibited a high channel activity immediately after excision and a considerable run-down over 2 to 6 min. The channel was sensitive to internal Ca^{2+} concentrations; addition of EDTA or EGTA to the bath, resulting in Ca^{2+} concentrations below 10 μM, gradually decreased the open probability of the channel (Fig. 2*c*) that was restored on readdition of Ca^{2+}.

Remarkably, addition of $InsP_4$ to inside-out patches displaying channel openings on activation by high Ca^{2+} concentrations (1 mM), evoked an immediate increase in the open probability (Fig. 3). $InsP_4$ (10–100 μM) increased channel activity (defined as the product of the number of channels, N, and the probability of channel opening, P_0) by a factor of 2 to 8 (mean 3.9 ± 2.0; $n = 12$). Activation by $InsP_4$ was reversible on washout (Fig. 3), but rundown of channel activity prevented intrapatch definition of the $InsP_4$ concentration-effect relation. $InsP_4$ (10–30 μM) increased channel activity at lower Ca^{2+} concentrations (0.47 μM) by a factor of 5.0 (±2.8; $n = 7$). No significant activation was induced by $InsP_4$ at a Ca^{2+} concentration of 0.1 μM. The limited analysis possible of channel kinetics suggested that the effects of $InsP_4$ were due to an increased frequency of openings rather than a prolongation of open time. In summary, basal channel activity scales with Ca^{2+} concentration and a minimum level of intracellular Ca^{2+} seems to be necessary for $InsP_4$-dependent channel activation.

In contrast to $InsP_4$, $InsP_3$ (50 and 100 μM) failed to induce any obvious increase in channel activity in 22 patches. In 10 patches, $InsP_4$, applied after $InsP_3$ stimulated the channel (Fig. 4). There was no indication that the effect of $InsP_4$ was enhanced by pretreatment with $InsP_3$ (Fig. 4*c*). 1,3,4,5,6-$InsP_5$ (500 μM; $n = 3$) enhanced channel activity at concentrations 50-fold higher than $InsP_4$ but not at 100 μM. Furthermore, GTP-γ-S (10 μM, in bath or pipette solution), alkalinization of the bath (pH 7.8), stretch (application of negative pressure up to −25 cm H_2O), and depolarization from −90 to −30 mV, all failed to activate the channel. Channel activity was blocked reversibly by bath application of 1–5 mM Ni^{2+}.

Although channel events were observed in excised patches in about one-third of experiments, channels were rarely detected in the cell-attached configuration in unstimulated cells. But

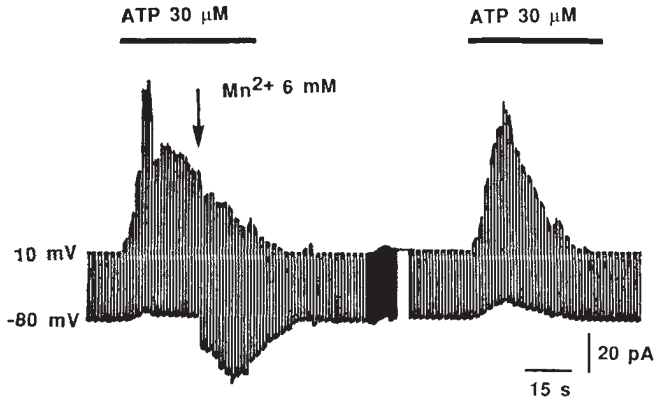

FIG. 1 Mn^{2+} influx into stimulated endothelial cells. An endothelial cell under perforated-patch whole-cell voltage clamp was alternately stepped from +10 to −80 mV each second. The cell was superfused with ATP (30 μM, bar), inducing a large outward current at +10 mV (largely calcium-activated K^+ current). During the first stimulation, 6 mM Mn^{2+} was added to the ATP solution perfusing the cell (for ~5 s from arrow), inducing an inward current at −80 mV. A recovery time of 5 min was allowed during the two stimulations. METHODS. Cultured endothelial cells from bovine aortae (subculture 13–30)[25] were grown on glass coverslips to subconfluence in Dulbecco's modified Eagle's medium with 20% fetal calf serum. The perforated-patch whole-cell voltage clamp technique[26] was done using nystatin as a pore-forming agent as described[9]. The patch-clamp pipette contained (in mM) KCl (40), K_2SO_4 (80), $MgCl_2$ (2), HEPES (15), pH 7.4, nystatin 0.1–0.3 mg ml^{-1}. Standard bath solution (SBS) contained NaCl (140), KCl (4), $CaCl_2$ (1), $MgCl_2$ (2), HEPES (10), glucose (5), pH 7.4. Superfusion with ATP solution (30 μM in $CaCl_2$-free SBS) was at 0.2 ml min^{-1} using a U-shaped glass capillary tube with an outlet hole placed next to the cell. Mn^{2+} was applied by introducing $CaCl_2$-free SBS with 30 μM ATP and 6 mM Mn^{2+} into a small tube inside the U-tube, with its outlet adjacent to the mouth of the U-tube. Records were filtered at 100 Hz. All experiments were done at 22 ± 2 °C.